# Engineering Launch Methods for Non-Spherical Hypervelocity Projectiles

**Daniel Rodriguez[(1)], Daniel Wentzel[(2)], Marcus Sandy[(1)], Donald J. Henderson[(2)], Arturo Pardo[(1)], Joshua E. Miller[(3)], Eric L. Christiansen[(4)], Bruce A. Davis[(3)] and Robert J. McCandless[(3)]**

[(1)] Sierra Lobo Inc., NASA White Sands Test Facility, 12600 NASA Rd., Las Cruces, NM 88012, United States of America, daniel.rodriguez-3@nasa.gov

[(2)] NASA White Sands Test Facility, Mail Code RF, 12600 NASA Rd., Las Cruces, NM 88012, United States of America, donald.j.henderson@nasa.gov

[(3)] Jacobs Technology, Inc., NASA Johnson Space Center, 2224 Bay Area Blvd., Houston, TX 77058, United States of America, joshua.e.miller@nasa.gov

[(4)] NASA Johnson Space Center, Mail Code XI5, 2101 NASA Parkway, Houston, TX 77058, United States of America, eric.l.christiansen@nasa.gov

**ABSTRACT**

The use of carbon-fiber-reinforced polymer (CFRP) in modern satellites has led to a significant amount of space debris, including fragments of CFRP and high-density metals such as steel and copper, produced during catastrophic breakup events. To address this issue, NASA's White Sands Test Facility (WSTF) has been developing the capability to launch "flake-like" and long "needle-like" projectiles. WSTF tested projectiles with different length-to-diameter ratios (L/D), impacting aluminum Whipple shields with thermal blankets on the outer surface, at velocities exceeding 6 km/s. The results of the study suggest that launching and imaging shaped projectiles at high velocities is feasible. Ongoing research is now focused on improving the techniques for launching and imaging shaped projectiles under hypervelocity conditions.

## 1 INTRODUCTION

The National Engineering Safety Center (NESC) issued a recommendation to categorize debris shapes and establish a correlation between characteristic length and mass/shape parameters. Collaborating with organizations such as the NASA Orbital Debris Program Office (ODPO), the United States Air Force, the Aerospace Corporation, and the University of Florida, an extensive dataset was gathered to characterize the shapes of a significant portion of this debris. It was determined that a considerable amount of this debris is primarily composed of carbon-fiber-reinforced polymer (CFRP) with length-to-diameter (L/D) ratios of approximately 1/3 (thin plate) or 3/1 (long rod) [1].

In June 2019, the Remote Hypervelocity Test Laboratory (RHTL) team received a request from the Johnson Space Center (JSC) Hypervelocity Impact Technology (HVIT) group to conduct experiments involving the launch of carbon, steel, and copper projectiles of diverse shapes. The overarching objective of these experiments was to establish the capacity for the successful launch and measurement of impact orientation of cylindrical projectiles at various L/D ratios, including 1/5 (thin plate), 2/3 (sphere equivalent mass), and 3/1 (long rod), targeting a designated shield.

The carbon material utilized in these series of tests was procured from CST The Composites Store, Inc. in the form of rods and sheets, and subsequently machined according to precise specifications. The resin employed for binding the carbon fiber was a high-performance Bisphenol A epoxy resin. The fiber volume fraction was determined to be 63%, and the calculated density of the composite material was 1.53 g/cm³.

## 2 HIGH-SPEED IMAGE SETUP

Two Shimadzu™ HyperVision HPV-X cameras, equipped with Nikon® AF Zoom-NIKKOR 80-200 mm Extra-Low Dispersion lenses, were employed for the purpose of recording both the in-flight orientation of the projectile and its post-impact damage. These high-speed cameras possess the capacity to capture footage at frame rates of up to 10 million frames per second (fps). However, for the specific requirements of these experiments, a frame rate of 2 million fps was deemed more suitable.
This selection was based on the benefits it offered in terms of enhanced image resolution and a greater quantity of images of the projectile over an extended time frame, consequently providing a more comprehensive and detailed understanding of its behavior. To optimize image brightness and exposure, an aperture of f/2.8 was employed, complemented by artificial lighting. Both cameras were strategically positioned orthogonal to each other, outside the target chamber. The precision of camera alignment was ensured through the use of an alignment fixture, focusing the cameras on the anticipated flight path of the projectile while maintaining their orthogonality. Additionally, the cameras were oriented at a 45-degree angle downward from the top of the target chamber (Fig. 1), with their focus directed at the projected flight path. A spatial fiducial was positioned to serve as a reference for scaling the camera images, providing a reliable frame of reference at the expected location of the projectile during its flight.

Achieving true orthogonal orientation for camera mounting presented a noteworthy challenge, necessitating the use of shimming techniques to offset the mounting hardware. To ensure the alignment of camera views converged at a common point on the spatial fiducial, an in-situ alignment tool was deployed, comprising five precision all-thread rods and a crosshair. Discrepancies between the true center, equidistant between the cameras, and the anticipated flight path of the projectile required adjustments to the mounting fixture and were meticulously accounted for in determining the in-flight orientation of the projectile.

Fine-tuning the imaging parameters aimed to attain an optimal balance between spatial resolution, temporal resolution, and focal depth within the limitations imposed by the equipment, lighting conditions, and the configuration of the target chamber. Spatial resolution was of particular significance, enhancing the pixel density within the imaged projectile and thereby enabling more accurate measurement of orientation and rotation. This resolution, however, is bounded by factors such as camera distance to the target and lens characteristics, including focal distance and zoom capability. Expanding the field of view (FOV) tends to reduce spatial resolution, while a narrower FOV enhances it but at the cost of a reduced number of frames capturing the projectile. This narrows the timeframe for image capture, compromises rotation measurement accuracy, and heightens sensitivity to velocity changes, potentially resulting in a failure to capture the projectile in flight.

Temporal resolution, governed by the frame rate, is crucial for capturing sufficient images to measure projectile orientation. Higher frame rates require increased light exposure, which can be compensated for with higher luminance. Finally, adjustments to the lens aperture were considered to maintain adequate exposure. A lower f-stop, allowing more light, does, however, reduce focal depth, potentially causing the projectile to fall out of focus when its flight path diverges from the expected trajectory, thereby impairing edge detection and study accuracy. Engineers and technicians dedicated their efforts to fine-tuning these parameters to ensure the acquisition of the highest quality images that would offer a precise assessment of projectile orientation.

In all experimental scenarios, camera activation was synchronized with a voltage signal generated by a photodiode situated in proximity to the stripper plate. The role of the stripper plate was to avert the sabot from making direct contact with the target, and upon impact, to facilitate the exchange of energy between it and the sabot, generating light. The pre-trigger timing for the cameras was computed by accounting for the distance between the stripper plate and the target, as well as the anticipated velocity of the projectile.


Fig. 1. High-speed imaging setup using frame-synchronized, ultrahigh-speed Shimadzu™ HyperVision HPV-X cameras located outside the target chamber.

## 3 DATA ANALYSIS

The primary objective of this study was to establish the capability to successfully launch cylindrical projectiles and accurately record their impact orientation, specifically focusing on various L/D ratios. A comprehensive summary of the materials utilized in this study, along with their respective dimensions, is provided in Table 1. Notably, more than 80% of the experiments employed CFRP due to its prevalence in the composition of most debris. The CFRP cylindrical projectiles employed throughout these experiments were crafted from pultruded rods. In contrast, disks were fabricated through turning or water jet cutting from CFRP sheets. A technical data summary of the materials utilized is presented in Table 2.

An area of particular concern revolved around the potential complexities arising during the launch process, largely attributed to the limited experience with testing carbon fiber. Carbon-fiber-reinforced polymer composites exhibit exceptional mechanical properties in the longitudinal direction but exhibit relatively poor transverse properties, constraining their utility in various structural applications. Previous experience at the White Sands Test Facility (WSTF) highlighted the inherent challenges associated with launching non-metallic materials, primarily due to their comparatively lower strength. The launch phase introduced a complex interplay of stresses, including shears, bending, and normal stresses, along with the differential inertial resistance between the projectile and the sabot. This combination could potentially result in projectile breakup, leading to the inadvertent damage of the barrel's inner bore and/or the target, thereby generating secondary debris. To mitigate these applied stresses, the study necessitated the implementation of optimization strategies for various gun parameters.

A series of experiments was conducted to gather empirical data and discern the key variables that enhance the likelihood of successfully launching cylindrical projectiles. The details of each trial performed in the course of this study are comprehensively summarized in Table 1. Following the formulation of a problem statement, four critical factors were identified and evaluated for their significant impact on the successful launch of shaped projectiles. These factors encompassed sabot design, projectile material, gun barrel quality, and flight range pressure. It was postulated that all these variables would exert a discernible influence on projectile delivery, necessitating the fine-tuning of these parameters to enhance this capability.

Table 1. Test Matrix of Shaped Projectile Study.

| Test # | Projectile Material | Diameter (mm) | Length (mm) | Mass (g) | Velocity (km/s) | Notes |
|---|---|---|---|---|---|---|
| 1 | CFRP | 5 | 3.33 | 0.1007 | 6.94 | Clean Test |
| 2 | CFRP | 5 | 3.33 | 0.1002 | 6.99 | Clean Test |
| 3 | CFRP | 5 | 3.33 | 0.0999 | 6.96 | Clean Test |
| 4 | CFRP | 6 | 1.2 | 0.0528 | 6.83 | Projectile Breakup |
| 5 | CFRP | 2.5 | 7.5 | 0.0564 | 6.97 | Projectile Impacted Stripper Plate |
| 6 | CFRP | 2.5 | 7.5 | 0.057 | 6.97 | Clean Test |
| 7 | CFRP | 2.5 | 7.5 | 0.0572 | 6.99 | Clean Test |
| 8 | CFRP | 3.45 | 2.3 | 0.0327 | 6.94 | Clean Test |
| 9 | CFRP | 7.94 | 1.58 | 0.1163 | 6.95 | Clean Test |
| 10 | CFRP | 7.94 | 1.58 | 0.1162 | 6.97 | Projectile Breakup |
| 11 | CFRP | 7.94 | 1.58 | 0.1166 | 6.96 | Projectile Impacted Stripper Plate |
| 12 | CFRP | 1.78 | 5.3 | 0.0204 | 7.00 | Clean Test |
| 13 | CFRP | 7.94 | 1.58 | 0.1161 | 6.99 | Projectile Breakup |
| 14 | CFRP | 7.94 | 1.58 | 0.117 | 5.96 | Clean Test |
| 15 | CFRP | 7.94 | 1.58 | 0.117 | 6.63 | Clean Test |
| 16 | CFRP | 7.94 | 1.58 | 0.117 | 6.84 | Projectile Impacted Stripper Plate |
| 17 | CFRP | 7.94 | 1.58 | 0.1146 | 7.28 | Projectile Impacted Stripper Plate |
| 18 | CFRP | 4 | 1.58 | 0.0302 | 6.63 | Clean Test |
| 19 | CFRP | 6 | 1.58 | 0.0663 | 6.55 | Impacted Stripper |
| 20 | Stainless Steel | 1.2 | 0.8 | 0.0071 | 6.88 | Clean Test |
| 21 | Stainless Steel | 1.2 | 0.4 | 0.0036 | 6.85 | Clean Test |
| 22 | Copper | 0.7 | 2 | 0.0071 | 6.85 | Clean Test |
| 23 | Copper | 0.7 | 2 | 0.0069 | 6.83 | Clean Test |
| 24 | CFRP | 1.8 | 5.27 | 0.02 | 6.97 | Clean Test |

## 4 SABOT DESIGN

By incorporating valuable insights gleaned from prior experiments conducted during the years 2007, 2008, 2009, and 2012 in the realm of shaped projectile testing, an innovative design was meticulously developed. This design immediately demonstrated its efficacy in achieving successful test results for projectile ratios of 2/3 and 3/1. The initial test design encompassed several significant features, which collectively contributed to its effectiveness.

A key optimization strategy involved fine-tuning the sabot length to strike a balance that minimized the overall launch package mass while avoiding sabot failure. Achieving a reduced launch package mass yields the advantage of requiring lower upstream pressure for achieving the desired projectile velocity, consequently resulting in a decrease in the magnitude of coupling stresses. This optimization further facilitates sabot separation, as a smaller mass carries diminished moment, rendering it more susceptible to the influence of aerodynamic effects. Moreover, additional modifications to the sabot pocket, aimed at attenuating the magnitude of forces transferred from the sabot to the projectile, hold the potential to further diminish the likelihood of potential failure.

Using a .50-caliber gun range, a deliberate decision was made to adopt a concise sabot length, meticulously constrained to not surpass 0.350 inches. This judicious choice substantially contributed to the overarching enhancement of the system's performance. Additionally, a purposeful modification was introduced through the incorporation of a strategically positioned divot at the rear of the pocket, effectively mitigating undesirable interactions between the sabot and the projectile during the critical phase of free-flight separation.

Furthermore, meticulous consideration was devoted to the precise positioning of the 35-degree face angle employed for drag separation, particularly in its interface with the projectile. Here, the projectile was positioned as far forward as feasible within the sabot while ensuring stable support during launch. This design choice allowed for the sabot to make contact with the projectile slightly above its midpoint, while avoiding the critical leading edge. This precaution served to prevent potential damage or weakening of the projectile, ensuring a secure hold at a structurally robust location.

These distinctive design attributes, when employed consistently across projectiles of various sizes, were found to contribute significantly to the overall success of the testing program.

The launch of a flat disk presents a particularly formidable challenge specifically the 1/5 (L/D) ratio. In 2009, a total of five attempts were undertaken with the 50-caliber launcher to launch disks composed of nylon and aluminum, each measuring 0.25 inches in diameter and 0.050 inches in thickness. The aluminum disks proved successful in reaching their intended target, whereas the nylon disks failed to do so. These unsuccessful attempts, however, yielded valuable insights and informative data.

Subsequently, in the year 2019, the initial endeavour to launch a carbon disk involved an attempt to replicate designs that had previously yielded successful outcomes in tests involving carbon materials. This approach was favored due to its efficiency in terms of machining time. However, the first attempt utilizing a CFRP disk resulted in projectile breakage (Fig.2). This occurred due to the application of squeeze forces during the launch that exceeded the structural integrity of the carbon disk.

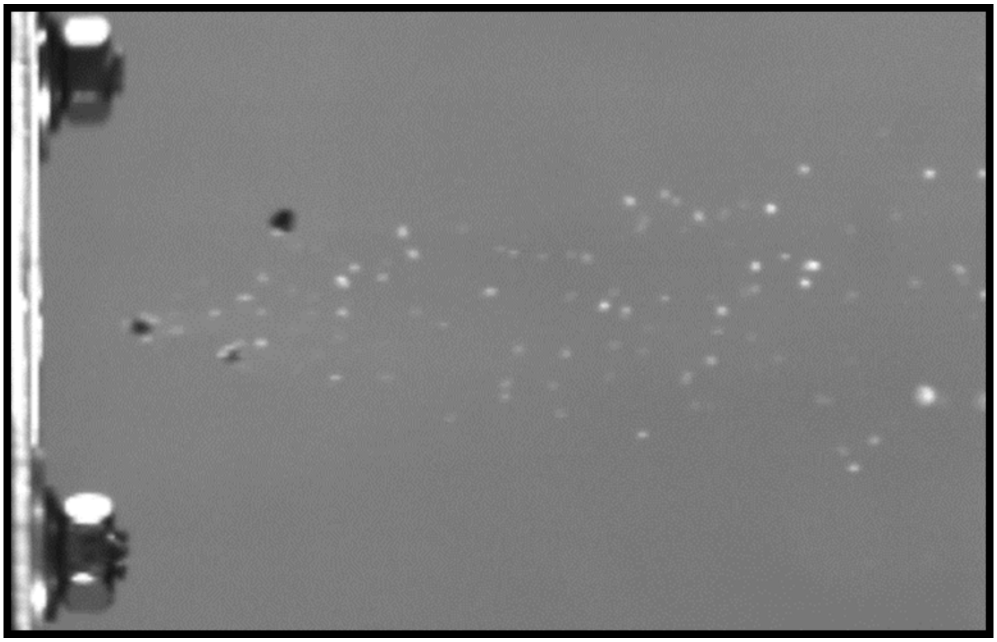

Fig. 2. Image of first 6 x 1.2 mm CFRP disk breakup machined from CFRP sheet with a length-to-diameter ratio of 1/5.

Following the occurrence of projectile breakup, a redesigned pocket was developed with the primary objective of mitigating the compressive forces acting on the projectile during the launch phase. The pocket within this sabot design was carefully engineered to redirect and disperse the squeezing forces away from the projectile during launch. However, it was essential to ensure that the fit between the pocket and the projectile was precisely calibrated.

An excessively tight fit between the pocket and the projectile risks inflicting damage upon the projectile due to excessive forces. Conversely, an overly loose fit raises the possibility of the projectile prematurely exiting the front of the sabot or descending to the side of the pocket during the launch cycle, potentially colliding with the stripper plate.

## 5 PROJECTILE MATERIAL

The long CFRP cylindrical projectiles employed in this series of tests were fabricated from pultruded rods. In contrast, the disks were manufactured through turning or water jet-cutting processes from CFRP sheets (Fig.3). For a comprehensive overview of the material properties and characteristics that were subjected to testing, Table 2 provides a summary of the technical data.

The act of launching CFRP projectiles, in comparison to metal projectiles, introduces an additional layer of complexity due to the asymmetry and comparatively diminished mechanical strength inherent to CFRP materials. Unlike metal projectiles, which possess greater resistance to deformation, a plastic sabot does not exert sufficient resistance to crush a metal projectile; however, it is sufficiently potent to deform or crush carbon fiber. Hence, it becomes imperative to prioritize a meticulous and dedicated focus on the design of the sabot when undertaking the task of launching CFRP materials.

Table 2. CFRP Technical Data.

| | |
|---|---|
| **Fiber Volume** | 63% |
| **Tensile Strength** | 2.4 Gpa |
| **Tensile Modulus** | 240 Gpa |
| **Compression Strength** | 1.00 Gpa |
| **Ultimate Elongation** | 1.10% |
| **Glass Transition Temp.** | 120 C |
| **Resin Type** | Bisphenol A |

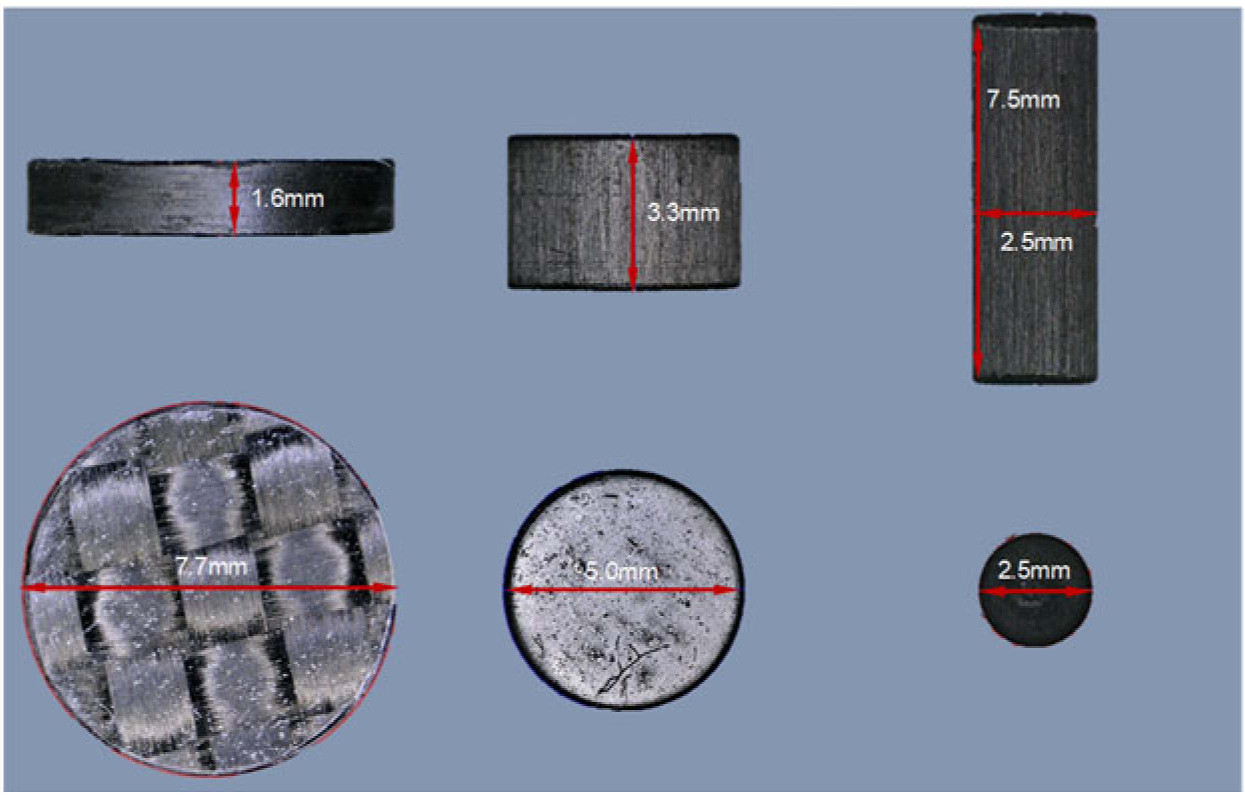


Fig. 3. Side and top images of cylindrical CFRP projectiles for different L/ D ratios.

## 6 GUN BARREL SELECTION

The utilization of a barrel that establishes a sturdy interface with the high-pressure segment of a two-stage gun stands out as a pivotal mechanism for the alleviation of potential projectile failures. The inclusion of a compact bore with a tapered entrance angle, precisely impedance-matched to the gun, affords the distinct benefit of enhancing power transmission without the need for supplementary energy to compensate for losses. This judicious optimization leads to a reduction in the magnitude of applied stresses, as it necessitates a lowered upstream pressure to attain the desired projectile velocity.

## 7 FLIGHT RANGE PRESSURE

Typically, large caliber guns necessitate a baseline level of downstream pressure to facilitate the aerodynamic separation of the sabot from the projectile. A reduction in the flight range pressure can be advantageous, as it serves to diminish inertial resistance to motion and gas friction, a particularly favorable condition for launching CFRP projectiles. However, it is important to exercise caution and avoid excessive reductions in flight range pressure, as this could impede the successful separation of the sabot. Within the framework of the conducted test series, the enhanced sabot design facilitated a deliberate reduction of flight range pressure by 40%. This reduction played a significant role in mitigating projectile ablation during flight (Fig.4).

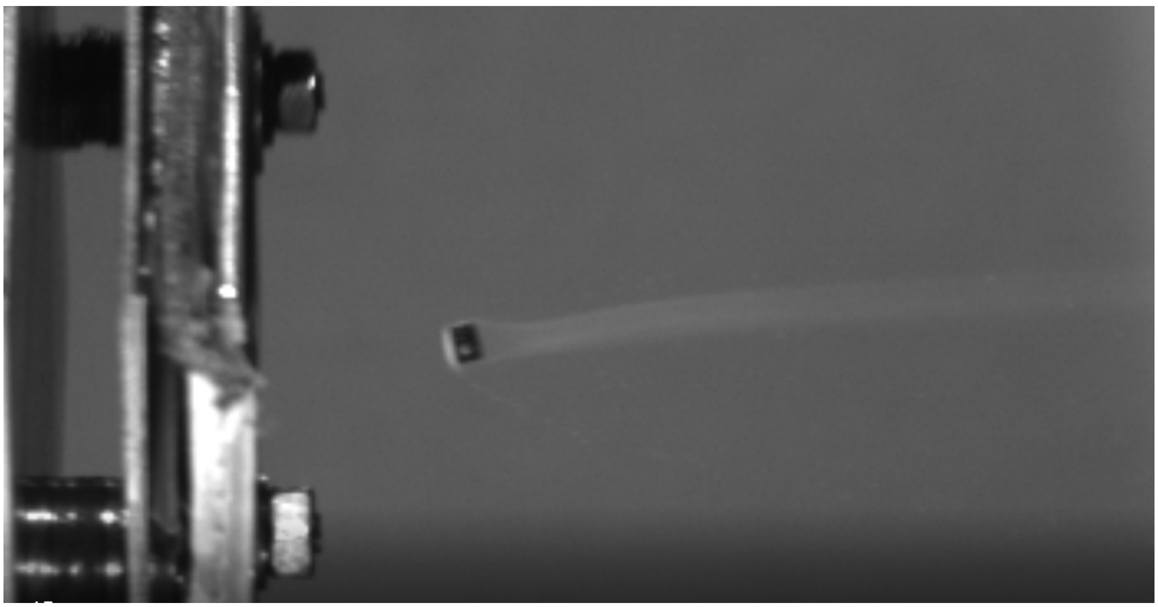

Fig. 4. Image of a 3.33 x 5 mm cylindrical CFRP machined from pultruded rods with a length-to-diameter ratio of 2/3 before impact.

One notable concern revolved around the issue of projectile mass loss resulting from friction drag. Figure 5 demonstrates the phenomenon of projectile ablation occurring prior to its impact with the target. It is noteworthy that all CFRP shots exhibited a certain degree of ablation. Ongoing efforts are dedicated to addressing this concern, and several potential strategies are under consideration. These include the application of a high-temperature coating to the projectile, the utilization of CFRP materials designed to withstand higher temperatures, and the reduction of aerodynamic friction through the adjustment of backfill pressure.

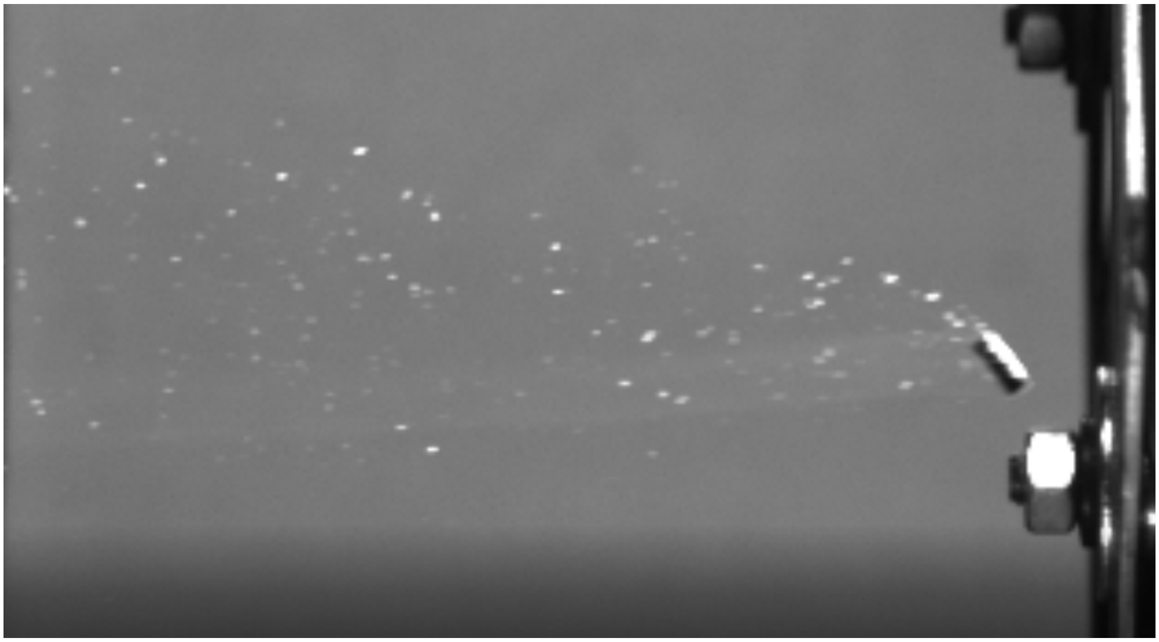

Fig. 5. Projectile ablation of CFRP rod.

## 8 CONCLUSION

The primary aim of this study was the development of innovative techniques to facilitate the launch of cylindrical projectiles at impact velocities approximating 7 km/s. The research has successfully demonstrated the feasibility of launching shaped projectiles, albeit with a need for further methodological refinement. The success rate achieved in this series of experiments stood at 66%, with unsuccessful attempts primarily attributed to either projectile failure or inadvertent collisions with the stripper plate.

Notably, the most challenging projectile shape to launch was the disk. Initial issues arose due to projectile compression within the sabot pocket, prompting subsequent modifications aimed at reducing applied stresses. However, these adjustments came at the expense of some aim-point accuracy. Consequently, the projectile consistently collided with the stripper, underscoring the critical requirement for an impeccably precise pocket fit.

Another significant insight gleaned from this study pertained to projectile ablation resulting from aerodynamic friction. This issue was observed across all CFRP shots and posed challenges that were not amenable to immediate control. Currently, ongoing endeavors are focused on the utilization of rifled barrels to facilitate sabot separation, thus eliminating the necessity for a fixed flight range pressure requirement. This strategic approach has effectively addressed the problem of ablation resulting from aerodynamic friction.

## 9 REFERENCES


1. J.E. Miller, “Development of analysis techniques for non-spherical hypervelocity impacts,” Proceedings of the 2022 Hypervelocity Impact Symposium, HVIS2022 (2022).
2. M. Polk, et. al., “Orbital debris assessment testing in the AEDC Range G,” Procedia Engineering, 103, pp. 490-498 (2015).
3. J.-C. Liou, et. al., “DebriSat-A planned laboratory-based satellite impact experiment for breakup fragment characterization,” International Astronautic Congress Proceedings, IAC-16.A6.2.8x35593 (2016).
4. N. Fitz-Coy, et. al., “Characterization of debris from the DebriSat hypervelocity test,” 66th International Astronautical Congress at Jerusalem, Israel, IAC-15-A6.2.9x30343, pp. 1-10 (2015).
5. H.M. Cowardin, et. al., “Optical characterization of DebriSat fragments in support of orbital debris environment models,” Advanced Maui Optical and Space Surveillance Technologies Conference proceedings, AMOS-2020.20115, (2020).
6. E.L. Christiansen, “Meteoroid/debris shielding,” NASA/TP-2003-210788 (2003).
7. J.E. Miller, “Simulation study of non-spherical, graphite-epoxy projectiles,” Proceedings of the 2019 Hypervelocity Impact Symposium, HVIS2019-044 (2019).